1521-0103/347/3/755–764$25.00
THE JOURNAL OF PHARMACOLOGY AND EXPERIMENTAL THERAPEUTICS

http://dx.doi.org/10.1124/jpet.113.208959
J Pharmacol Exp Ther 347:755–764, December 2013

Pharmacokinetic Assessment of Efflux Transport in Sunitinib Distribution to the Brain

Rajneet K. Oberoi, Rajendar K. Mittapalli, and William F. Elmquist

Department of Pharmaceutics, Brain Barriers Research Center, University of Minnesota, Minneapolis, Minnesota

Received August 19, 2013; accepted October 10, 2013

ABSTRACT

This study quantitatively assessed transport mechanisms that limit the brain distribution of sunitinib and investigated adjuvant strategies to improve its brain delivery for the treatment of glioblastoma multiforme (GBM). Sunitinib has not shown significant activity in GBM clinical trials, despite positive results seen in preclinical xenograft studies. We performed in vivo studies in transgenic Friend leukemia virus strain B mice: wild-type, *Mdr1a/b(−/−)*, *Bcrp1(−/−)*, and *Mdr1a/b(−/−)Bcrp1(−/−)* genotypes were examined. The brain-to-plasma area under the curve ratio after an oral dose (20 mg/kg) was similar to the steady-state tissue distribution coefficient, indicating linear distribution kinetics in mice over this concentration range. Furthermore, the distribution of sunitinib to the brain increased after administration of selective P-glycoprotein (P-gp) or breast cancer resistance protein (Bcrp) pharmacological inhibitors and a dual inhibitor, elacridar, comparable to that of the corresponding transgenic genotype. The brain-to-plasma ratio after coadministration of elacridar in wild-type mice was ∼12 compared with ∼17.3 in *Mdr1a/b(−/−)Bcrp1(−/−)* mice. Overall, these findings indicate that there is a cooperation at the blood-brain barrier (BBB) in restricting the brain penetration of sunitinib, and brain delivery can be enhanced by administration of a dual inhibitor. These data indicate that the presence of cooperative efflux transporters, P-gp and Bcrp, in an intact BBB can protect invasive glioma cells from chemotherapy. Thus, one may consider the use of transporter inhibition as a powerful adjuvant in the design of future clinical trials for the targeted delivery of sunitinib in GBM.

Introduction

Glioblastoma multiforme (GBM) is an aggressive tumor with a median survival of 12.6 months with treatment (Louis et al., 2007). Progression of glioma is dependent on a rich blood supply accomplished by angiogenesis (Brem et al., 1992; Tuettenberg et al., 2006), a process mediated by vascular endothelial growth factor receptor (VEGFR), platelet-derived growth factor receptor (PDGFR), basic fibroblast growth factor, and epidermal-derived growth factor receptor (Tuettenberg et al., 2006; Wong et al., 2009). Antiangiogenic therapy is an important treatment option for GBM, in addition to cytotoxic therapy with temozolomide. Bevacizumab (Avastin), an anti-VEGF monoclonal antibody, was approved in May 2009 for GBM (Cohen et al., 2009). Since then, several targeted agents, such as tyrosine-kinase inhibitors (TKIs), have been tested in clinical trials, alone and in combination with other anticancer therapies. None of these treatment regimens has shown significant efficacy in GBM patients (di Tomaso et al., 2011; Wick et al., 2011), leaving several unresolved questions such as whether the drugs themselves are ineffective or if the delivery of a possibly effective drug is inadequate or both.

Effective delivery of drugs for the treatment of brain disorders has always been a challenging task due to the presence of the blood-brain barrier (BBB). The BBB comprises endothelial cells annealed by tight junctions, which is further complicated by the presence of active efflux transporters. The ATP-binding cassette (ABC) family of transporters include P-glycoprotein (P-gp; ABCB1) and breast cancer resistance protein (BCRP; ABCG2), two major efflux transporters present in the luminal side of the BBB. These transporters work in tandem to restrict delivery of several therapeutics into the brain (Agarwal et al., 2011a; Agarwal and Elmquist, 2012).

The microvasculature within a brain tumor is heterogeneous. The tumor core has some degree of necrosis and is highly permeable (Horowitz et al., 1983), whereas the brain adjacent to the core may have a slightly higher permeability than normal brain (Levin et al., 1975). The core, visualized by magnetic resonance imaging, is often removed during

This work was supported by National Institutes of Health National Cancer Institute [Grants CA138437 and NS077921]; and the Ronald J. Sawchuk Fellowship in Pharmacokinetics, Department of Pharmaceutics, University of Minnesota (to R.K.O.).
dx.doi.org/10.1124/jpet.113.208959.

ABBREVIATIONS: ABC, ATP-binding cassette; AUC, area under the curve; BBB, blood-brain barrier; Bcrp, breast cancer resistance protein; DTI, drug-targeting index; FVB, Friend leukemia virus strain B; GBM, glioblastoma multiforme; GF120918, elacridar, *N*-(4-[2-(6,7-dimethoxy-3,4-dihydro-1*H*-isoquinolin-2-yl)ethyl]-5-methoxy-9-oxo-10*H*-acridine-4-carboxamide; Ko143, (3*S*,6*S*,12a*S*)-1,2,3,4,6,7,12,12*a*-octahydro-9-methoxy-6-(2-methylpropyl)-1,4-dioxopyrazino(1′,2′:1,6) pyrido(3,4-*b*)indole-3-propanoic acid 1,1-dimethylethyl ester; K_p, tissue partition coefficient; LY335979, (zosuquidar), (*R*)-4-((1*aR*,6*R*,10*bS*)-1,2-difluoro-1,1*a*,6,10*b*-tetrahydrodibenzo-(*a*,*e*)cyclopropa(*c*)cycloheptan-6-yl)-α-((5-quinoloyloxy) methyl)-1-piperazine ethanol, trihydrochloride; MDR1, gene encoding the human P-glycoprotein (multidrug resistance protein 1); PDGFR, platelet-derived growth factor receptor; P-gp, P-glycoprotein; SU112468, sunitinib, *N*-(2-diethylaminoethyl)-5-[(*Z*)-(5-fluoro-2-oxo-1*H*-indol-3-ylidene)methyl]-2,4-dimethyl-1*H*-pyrrole-3-carboxamide; TKI, tyrosine-kinase inhibitor; T_{max}, time to reach C_{max}; VEGFR, vascular endothelial growth factor receptor.

resection; however, the tumor cells adjacent to the core are found in regions with a relatively intact BBB, and are capable of causing tumor recurrence. Furthermore, some tumor cells infiltrate into distant sites of the brain to form a sanctuary of tumor cells, thus making GBM, in essence, a "whole brain" disease (Agarwal et al., 2011b). The tumor and BBB characteristics work in tandem to present a real challenge in achieving adequate drug delivery throughout the brain, which would yield a treatment that will be most likely to result in a longer progression-free survival in GBM (Agarwal et al., 2011b).

Sunitinib (*N*-(2-diethylaminoethyl)-5-[(*Z*)-(5-fluoro-2-oxo-1*H*-indol-3-ylidene)methyl]-2,4-dimethyl-1*H*-pyrrole-3-carboxamide; SU112468; Sutent; molecular mass 532.6 g/mol; molecular formula, C26H33FN4O7) is an orally active TKI with activity against VEGFR1–3 and PDGFR-α/β receptors, which are overexpressed in gliomas (Faivre et al., 2007). Preclinical studies have shown significant antitumor and antiangiogenic activity of sunitinib (Zhou et al., 2008; Zhou and Gallo, 2009). However, recent clinical trials have been disappointing (Neyns et al., 2011; Pan et al., 2012). One possibility for these conflicting results could be attributed to the lack of adequate drug delivery, mediated by the efflux transporters at the BBB. Sunitinib is known to interact with P-gp and Bcrp at the BBB (Dai et al., 2009; Hu et al., 2009; Shukla et al., 2009).

Recently, Tang et al. (2012) reported that sunitinib is transported in vitro by human ABCB1 (MDR1, multidrug resistance protein 1, P-gp) and ABCG2 (BCRP) and murine ABCG2 (Bcrp), but not by human ABCC2 (multidrug resistance associated protein 2, MRP2). They showed that single knockout of efflux transporters, P-gp or Bcrp, did not result in a profound increase in the brain accumulation of sunitinib when given as a single oral dose of 10 mg/kg; however, absence of both transport systems (*Abcb1a/1b/Abcg2*$^{-/-}$) resulted in a 23-fold increase in brain penetration. Furthermore, administration of a high dose of an inhibitor of both P-gp and Bcrp, elacridar, resulted in a 12-fold increase in brain accumulation of sunitinib, comparable to the levels observed in *Abcb1a/1b/Abcg2*$^{-/-}$ mice when examined at a single time point (Tang et al., 2012).

Therefore, the primary aim of this investigation was to study the interaction of sunitinib with P-gp and Bcrp at the BBB and quantitatively assess, using basic pharmacokinetic principles, the brain partitioning. We further proposed strategies to improve the brain distribution of sunitinib. We determined how assessment of brain partitioning at any single time point can lead to misinterpretation of the influence of efflux mechanisms; however, this assessment can be achieved at transient steady state. A novel aspect of this study is the inhibition of remaining P-gp and Bcrp in Bcrp knockout and P-gp knockout mice, respectively. This is important, especially for a tumor such as glioma, which is highly invasive in nature and has a greater tendency to infiltrate into the normal regions of the brain. Thus, subtherapeutic concentrations in the regions where the BBB has intact tight junctions, in conjunction with efflux transporters, can lead to decreased delivery, and hence efficacy of the targeted therapeutic agent.

Materials and Methods

Chemicals and Reagents. Sunitinib malate and dasatinib free base were purchased from LC Laboratories (Woburn, MA). Elacridar [GF120918; *N*-(4-[2-(6,7-dimethoxy-3,4-dihydro-1*H*-isoquinolin-2-yl)ethyl]-5-methoxy-9-oxo-10*H*-acridine-4-carboxamide and Ko143 [(3*S*,6*S*,12a*S*)-1,2,3,4,6,7,12,12*a*-octahydro-9-methoxy-6-(2-methylpropyl)-1,4-dioxopyrazino(1′,2′:1,6) pyrido(3,4-*b*)indole-3-propanoic acid 1,1-dimethylethyl ester] were purchased from Toronto Research Chemicals, Inc. (North York, ON, Canada). Zosuquidar [LY335979; (zosuquidar), (*R*)-4-((1a*R*,6*R*,10bS)-1,2-difluoro-1,1a,6,10btetrahydrodibenzo-(*a*,*e*)cyclopropa(c)cycloheptan-6-yl)-α-((5-quinoloyloxy) methyl)-1-piperazine ethanol, trihydrochloride;] was a gift from Eli Lilly & Co. (Indianapolis, IN). All other reagents and chemicals were of high-performance liquid chromatography grade and were purchased from Sigma-Aldrich (St. Louis, MO).

Animals. In vivo studies were performed in the Friend leukemia virus strain B (FVB) mouse strain of either sex and included the following types of mice: wild-type and transgenic mice in which the gene for P-gp [*Mdr1a/b*(−/−) knockout mice], Bcrp [*Bcrp1*(−/−) knockout mice], and both P-gp and Bcrp [*Mdr1a/b*(−/−) *Bcrp1*(−/−) or "triple knockout" mice] was knocked out, obtained from Taconic Farms (Germantown, NY). All mice were 8–10 weeks old and were maintained under temperature-controlled conditions with a 12-hour dark/12-hour light cycle. Mice were handled according to the guidelines set by the National Institutes of Health, and all experiments were conducted in accordance with the Institutional Animal Care and Use Committee of the University of Minnesota.

Plasma and Brain Pharmacokinetics after Oral Administration. The sunitinib dosing solutions for all in vivo studies were prepared as a stable suspension in 1% carboxymethylcellulose on the day of the experiment. All mice were administered 20 mg/kg by oral gavage and were euthanized using a carbon dioxide chamber at the desired time point. Since sunitinib exhibits light-sensitive diastereoisomerism (de Bruijn et al., 2010), all experiments and sample analyses were performed under light-protected conditions.

In the oral dosing study, wild-type, *Mdr1a/b*(−/−), *Bcrp1*(−/−), and *Mdr1a/b*(−/−)*Bcrp1*(−/−) mice were administered a 20 mg/kg sunitinib suspension via oral gavage. Blood and brain samples were harvested at predetermined time points, i.e., 0.5, 1, 2, 4, 6, 11, 16, and 22 hours postdose (n = 3–4 at each time point). Following euthanasia, blood was collected via cardiac puncture and immediately transferred to tubes containing 20 μl of 100 U/ml heparinized saline. Plasma was obtained by centrifugation at 4°C at 3500 rpm for 15 minutes. Whole brains were rapidly removed, rinsed with ice-cold buffer, and blotted with tissue paper to remove superficial blood vessels, followed by flash freezing in liquid nitrogen. Brains were transferred to preweighed tubes and plasma, and brain samples were stored at −80°C until analysis.

On the day of the analysis, brain samples were thawed at room temperature, and brain weights were determined. Brains were homogenized using 3 volumes of ice-cold 5% bovine serum albumin prepared in phosphate-buffered saline (pH 7.4) using a tissue homogenizer (PowerGen 125; Thermo Fisher Scientific, Pittsburgh, PA).

Previously, we have determined that the brain vascular space in FVB mice is 1.4% of the whole brain volume (Dai et al., 2003); therefore, we used this value to correct all brain concentrations for the residual drug in the brain vasculature.

Steady-State Brain Distribution of Sunitinib. The steady-state brain-to-plasma ratio or the "tissue partition coefficient" (K_p) was determined for sunitinib by measuring the plasma and brain concentrations in wild-type, *Mdr1*(−/−), *Bcrp1*(−/−), and *Mdr1a/b*(−/−)*Bcrp1*(−/−) mice using Alzet osmotic minipumps (Durect Corporation, Cupertino, CA), as described previously for sunitinib (Dudek et al., 2013). In brief, 30 mg of sunitinib was dissolved in 1 ml of dimethylsulfoxide, and osmotic minipumps (model 1003D) were loaded with 100 μl. The pumps were equilibrated by immersing them overnight in saline at 37°C under light-protected conditions. On the day of the experiment, mice were anesthetized with isoflurane (Boynton Health Service Pharmacy, University of Minnesota, Minneapolis, MN), and the primed pumps were surgically implanted in the peritoneal cavity of the mice, after which the mice were allowed to recover on a heated pad. Each minipump is designed to operate at

a flow rate of 1 μl/h, which in this case yields a constant intraperitoneal infusion rate of 30 μg/h. After 48 hours (approximately 24 half-lives), animals were euthanized, and brain and blood samples were harvested as described earlier. A 48-hour infusion was sufficient to achieve steady state as both the plasma and brain half-lives were approximately 2 hours. Plasma and brain samples were stored at −80°C until the day of analysis. On the day of the analysis, brains were prepared for analysis as described earlier.

Inhibition of P-gp and/or Bcrp1. The influence of selective or dual pharmacological inhibition of P-gp and Bcrp on the brain distribution of sunitinib was examined by pretreating FVB wild-type mice with selective inhibitors of P-gp (zosuquidar, LY335979) (Shepard et al., 2003), Bcrp (Ko143) (Allen et al., 2002), and a dual inhibitor of P-gp/Bcrp (elacridar, GF120918) (Maliepaard et al., 2001; Hubensack et al., 2008). Zosuquidar was administered at a dose of 25 mg/kg, and both Ko143 and elacridar were administered at doses of 10 mg/kg (vehicle: 40% dimethylsulfoxide, 40% propylene glycol, 20% saline). All inhibitors were administered via intravenous route, 30 minutes prior to sunitinib dosing (20 mg/kg) via oral gavage. Mice were sacrificed 1 hour after sunitinib dosing, and blood and brain specimens were collected and prepared for analysis as described earlier. To further delineate the role of P-gp and Bcrp in regulating the brain distribution of sunitinib at the mouse BBB, we studied the effect of selective pharmacological inhibitors in transgenic mice; therefore, P-gp knockout mice [*Mdr1a/b(−/−)*] were administered a Bcrp-selective inhibitor, Ko143 (10 mg/kg); Bcrp knockout mice [*Bcrp1(−/−)*] were administered a P-gp–selective inhibitor, zosuquidar (25 mg/kg); and FVB wild-type mice were administered both zosuquidar and Ko143 intravenously 30 minutes prior to the sunitinib oral dose (20 mg/kg). Mice were sacrificed 1 hour after sunitinib dosing, and blood and brain specimens were collected and stored at −80°C until analysis.

Furthermore, we compared the brain concentrations and brain-to-plasma concentration ratios at the 1-hour time point following pharmacological inhibition with those obtained at the 1-hour time point in genetically altered mice, i.e., the *Mdr1a/b(−/−)*, *Bcrp1(−/−)*, and *Mdr1a/b(−/−)Bcrp1(−/−)* mice after oral administration. Moreover, given that these brain distribution data are often reported in the literature at a single time point postdose, these experiments allow us to compare single time point brain distribution (brain-to-plasma concentration ratios at a single time point) with the steady-state concentration ratios and the area under the curve (AUC) ratios from time zero to infinity.

Data Analysis. Estimation of pharmacokinetic parameters and metrics was accomplished using Phoenix WinNonlin version 6.3 using noncompartmental estimation methods (Pharsight, Mountain View, CA). C_{max} and T_{max} were direct measurements obtained as the maximum observed concentration and the time to reach C_{max}, respectively. The area under the concentration-time profile (AUC) was calculated up to the last measured concentration using log-linear trapezoidal approximation ($AUC_{0\text{-tlast}}$), with an area extrapolation to time infinity in the terminal phase by adding C_{last}/λ_z, where λ_z is the terminal rate constant of the drug from plasma or brain, which was calculated from the last three to five data points of the respective concentration-time profiles. An extension of the method by Nedelman and Jia (1998) was used to analyze data using a sparse sampling method, and to estimate variance in area under the concentration-time profile from time 0 to the last measurable time point. The percentage of extrapolated AUC was less than 2% for all four groups for both plasma and brain. In addition, we assessed the transient steady-state kinetics of sunitinib. A transient steady state in the brain concentration of sunitinib occurs when the brain concentration is at maximum ($C_{max\ brain}$). At that time, the rate of change of drug concentration in the brain is zero. That is, a transient steady state is determined by the ratio of maximum observed brain concentration (C_{max}) to the corresponding plasma concentration at that time point. The AUC brain-to-plasma ratio and the "transient" steady-state ratio were compared with the steady-state brain-to-plasma ratio obtained after a continuous intraperitoneal infusion lasting 48 hours. We also determined brain-to-plasma concentration ratios at all measured time points in all genotypes. Furthermore, a drug-targeting index (DTI) of sunitinib was determined for both efflux transporters as AUC brain-to-plasma ratios of the "treatment" groups (P-gp knockout, Bcrp knockout, or triple knockout) divided by the AUC brain-to-plasma ratios of the control group, in this case the AUC brain-to-plasma ratio in FVB wild-type mice, written as

$$\mathrm{DTI} = \left[\mathrm{AUC_{brain}}/\mathrm{AUC_{plasma}}\right]_{,\text{knockout}} / \left[\mathrm{AUC_{brain}}/\mathrm{AUC_{plasma}}\right]_{,\text{wild-type}}$$

Liquid Chromatography–Tandem Mass Spectrometry Analysis. Quantitative determination of sunitinib concentrations in mouse plasma and brain tissue homogenate was performed using high-performance liquid chromatography–tandem mass spectrometry according to the method previously described (Oberoi et al., 2013). In brief, on the day of the analysis, samples were thawed at room temperature, protected from light. Brain samples were homogenized with 3 volumes of 5% ice-cold bovine serum albumin in phosphate-buffered saline (pH 7.4). One hundred microliters of plasma and 200 μl of brain homogenate were transferred to microcentrifuge tubes containing 100 μl of internal standard, dasatinib (2000 ng/ml). Samples were extracted by adding 1 ml of ice-cold ethyl acetate and vigorously shaken for 5 minutes, followed by centrifugation at 4°C at 7500 rpm for 10 minutes. Seven hundred fifty microliters of the supernatant was transferred to microcentrifuge tubes and dried under a gentle stream of nitrogen. Dried samples were reconstituted in 100 μl of mobile phase (70:30:0.1, v/v %, 20 mM ammonium formate, pH 3.5: acetonitrile: formic acid) and transferred to amber-colored glass vials. Five microliters of the sample was injected into liquid chromatography–tandem mass spectrometry. The chromatographic system consisted of an Agilent Technologies model 1200 separation system (Agilent Technologies, Santa Clara, CA). Separation of the analyte was achieved on a ZORBAX XDB Eclipse C_{18} column (4.6 × 50 mm, 1.8 μm; Agilent Technologies). The liquid chromatography-system was interfaced with a TSQ Quantum triple quadrupole mass spectrometer (Thermo Finnigan, San Jose, CA) equipped with selected reaction monitoring mode by an electrospray ionization source operated in positive ion mode at a spray voltage of 4000 V. The mobile phase flow rate was 0.25 ml/min and the total run time was 13 minutes. Data acquisition and analysis was performed using the Xcalibur software, version 2.0.7. (Thermo Finnigan, San Jose, CA). The mass-to-charge transitions programmed in the spectrometer were (399→283) and (488→401) for analyte sunitinib and internal standard, dasatinib, respectively.

Statistical Analysis. Unpaired two-sample t tests were used to test for statistical significance between two groups. One-way analysis of variance, followed by Bonferroni's test, was used to test for significance among multiple groups. Significance was declared at $P < 0.05$ for all tests (GraphPad Prism 5.01; GraphPad Software, Inc., San Diego, CA).

Results

Sunitinib Pharmacokinetics in Plasma and Brain after Oral Administration. Sunitinib plasma and brain concentration-time profiles were determined in wild-type, *Mdr1a/b(−/−)*, *Bcrp1(−/−)*, and *Mdr1a/b(−/−)Bcrp1(−/−)* mice after a single oral dose of 20 mg/kg sunitinib. The plasma and brain concentrations in the wild-type mice at the 22-hour time point were below the limit of quantification (1.95 ng/ml) and therefore were not considered in the pharmacokinetic analyses.

Plasma concentrations (and hence the AUCs in plasma) were not statistically different among the four genotypes. This suggests that absence of P-gp and/or Bcrp does not influence the systemic pharmacokinetics (total body clearance or volume of distribution overall) of sunitinib. The apparent oral

clearances observed among the genotypes were similar. The apparent oral clearances of sunitinib in wild-type, *Mdr1a/b(−/−)*, *Bcrp1(−/−)*, and *Mdr1a/b(−/−)Bcrp1(−/−)* were 4.6, 4.1, 5.1, and 6.5 ml/min, respectively. This is reflected in similar areas under the plasma concentration-time profiles among each group (AUC plasma) (Fig. 1A; Table 1). However, the brain concentrations varied greatly among the genotype groups. In the wild-type mice, the brain concentrations were lower than the plasma concentrations at all measured time points, indicating limited delivery of sunitinib into the brain. Brain concentration-time profiles in Bcrp knockout mice and P-gp knockout mice closely followed concentrations corresponding to the plasma. This indicates that Bcrp and P-gp alone do not dramatically affect the brain distribution of sunitinib. However, the brain concentrations in the triple knockout mice were significantly greater than the plasma concentrations at all measured time points ($P < 0.05$), indicating that, as with many other TKIs, sunitinib brain distribution is influenced by both P-gp and Bcrp acting in concert at the BBB (Fig. 1B) (Chen et al., 2009; Lagas et al., 2009; Polli et al., 2009; Agarwal et al., 2011a; Poller et al., 2011; Agarwal and Elmquist, 2012). Noncompartmental analysis of all four concentration-time profiles indicated that the terminal half-life in plasma was similar to the terminal half-life in the brain within each group. The half-life in plasma ranged from 1.8 to 3.0 hours, whereas the half-life in the brain ranged from 2.0 to 3.2 hours (Table 1). Although the AUC in plasma was not different between groups, significant differences were observed in the brain AUCs ($AUC_{0\text{-tlast}}$) in all knockout mice compared with the wild-type mice. This indicates that the efflux transporters influence sunitinib brain distribution between groups; a slight difference was observed in the P-gp and BCRP knockout animals, but with a much more pronounced effect in the triple knockout animals. The maximum observed concentration in the brain ($C_{\text{max brain}}$) was also significantly different between all groups of mice. The $C_{\text{max brain}}$ in the wild-type (0.13 ± 0.04 μg/g) was lower than that observed in *Bcrp1(−/−)* mice (0.20 ± 0.02 μg/g), *Mdr1a/b(−/−)* mice (0.52 ± 0.14 μg/g), and *Mdr1a/b(−/−)Bcrp1(−/−)* mice (4.9 ± 0.7 μg/g). The area under the brain concentration-time profile ($AUC_{0\text{-}\infty,\text{ brain}}$) was 37.4-fold higher in *Mdr1a/b(−/−)Bcrp1(−/−)* mice compared with wild-type mice, whereas the AUC brain was 4.75-fold higher in *Mdr1a/b(−/−)* mice and 2.08-fold higher in Bcrp1(−/−) mice compared with the wild-type mice (Table 1).

The resulting AUC brain-to-plasma ratio, also known as tissue K_p (brain-to-plasma partition coefficient), was 0.42 in the wild-type mice, suggesting that sunitinib has, compared with many other TKIs (Agarwal et al., 2011c; Minocha et al., 2012b,a; Agarwal et al., 2013), a greater partitioning in the brain. However, in the absence of both P-gp and Bcrp [*Mdr1a/b(−/−)Bcrp1(−/−)* mice], the AUC brain-to-plasma ratio is 20.5, whereas in *Mdr1a/b(−/−)* and *Bcrp1(−/−)* mice, the AUC brain-to-plasma ratio was 1.61 and 0.88, respectively. These results indicate that both P-gp and Bcrp work in cooperation to efflux sunitinib out of the brain. This could impact the drug levels in the brain for treatment of brain tumors, both primary and metastatic. The DTI of sunitinib was calculated as the ratio of AUC brain-to-plasma ratios in the transgenic mice divided by the same ratio in the control group, which in this case comprised the wild-type mice. Based on the mean $AUC_{0\text{-}\infty}$ values, the observed DTI values were 3.9 for *Mdr1a/b(−/−)*, 2.1 for *Bcrp1(−/−)*, and 48.9 for *Mdr1a/b(−/−)Bcrp1(−/−)*. This indicates a great influence of the efflux transporters in limiting the brain targeting of sunitinib (Table 1). These results closely follow

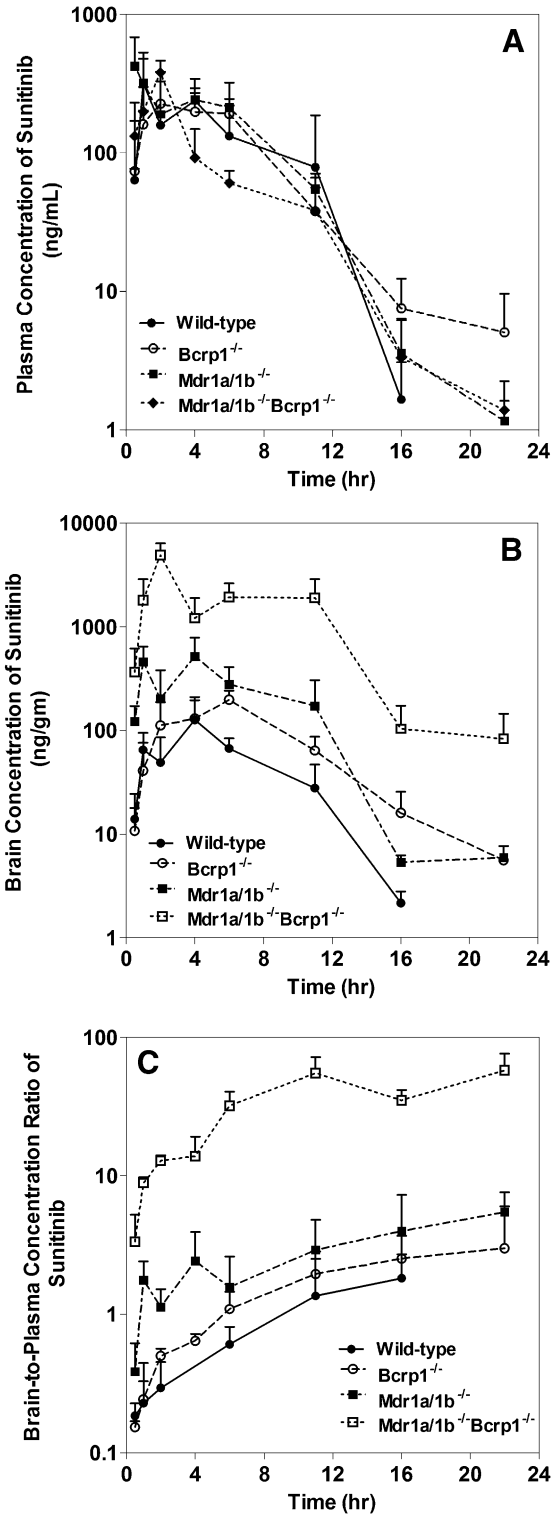

Fig. 1. (A) Plasma concentration-time profiles of sunitinib after a single oral dose (20 mg/kg) in FVB wild-type, *Mdr1a/b(−/−)*, *Bcrp1(−/−)*, and *Mdr1a/b(−/−)Bcrp1(−/−)* mice. (B) Corresponding brain concentration-time profiles of sunitinib after a single oral dose (20 mg/kg) in FVB wild-type, *Mdr1a/b(−/−)*, *Bcrp1(−/−)*, and *Mdr1a/b(−/−)Bcrp1(−/−)* mice. (C) Brain-to-plasma ratios with time in wild-type, *Mdr1a/b(−/−)*, *Bcrp1(−/−)*, and *Mdr1a/b(−/−)Bcrp1(−/−)* mice.

TABLE 1

Plasma and brain pharmacokinetic parameters determined by noncompartmental analysis after the administration of a single oral dose of sunitinib (20 mg/kg) in wild-type, *Mdr1a/b(−/−)*, *Bcrp1(−/−)*, and *Mdr1a/b(−/−)Bcrp1(−/−)* mice

Results are expressed as the mean ± S.D. (n = 3–4).

Parameter	FVB Wild Type	*Mdr1a/b(−/−)*	*Bcrp1(−/−)*	*Mdr1a/b(−/−)Bcrp1(−/−)*
Plasma				
C_{max} (μg/ml)	0.32 ± 0.08	0.42 ± 0.13	0.225 ± 0.09	0.38 ± 0.04
Half-life (h)[a]	1.8	2.1	3.0	2.8
T_{max} (h)	1	0.5	2	2
CL/F (ml/min)	4.6	4.1	5.1	6.5
$AUC_{0\text{-tlast}}$ (h-μg/ml)	1.85 ± 0.36	2.26 ± 0.26	1.81 ± 0.20	1.39 ± 0.12
$AUC_{0\text{-}\infty}$ (h-μg/ml)	1.85	2.27	1.83	1.40
Brain				
C_{max} (μg/ml)	0.13 ± 0.04	0.52 ± 0.14	0.20 ± 0.02	4.92 ± 0.74
Half-life (h)[a]	2.0	2.5	3.2	3.0
T_{max} (h)	4	4	6	2
$AUC_{(0\text{-tlast})}$ (h-μg/ml)	0.76 ± 0.11	3.63 ± 0.15	1.58 ± 0.15	28.43 ± 3.10
$AUC_{(0\text{-}\infty)}$ (h-μg/ml)	0.77	3.65	1.61	28.8
Brain/plasma ratio				
AUC_{Brain}/AUC_{Plasma}	0.42	1.61	0.88	20.53
DTI		3.9	2.1	48.9

CL/F, apparent clearance.
[a]Time taken to reach one-half of its steady-state value.

the pattern previously observed for several TKIs, where a greater than additive effect of P-gp and Bcrp is observed (Lagas et al., 2009; Polli et al., 2009). Our results indicate that the efflux activity with *Mdr1a/b(−/−)* mice and *Bcrp1(−/−)* mice is a combined effect since we determined that P-gp efflux activity [DTI for *Mdr1a/b(−/−)* mice] was 3.8-fold and Bcrp efflux activity [DTI for *Bcrp1(−/−)* mice] was 2.4-fold. Therefore, it is hard to conclusively say whether P-gp or Bcrp makes a greater contribution to the in vivo efflux clearance of sunitinib from the brain. Nevertheless, it is clear that both transporters work in tandem at the BBB to efflux sunitinib from the brain, and the action of both transporters must be inhibited to significantly improve the distribution of sunitinib to the brain.

The brain-to-plasma concentration ratios versus time for all genotypes are shown in Fig. 1C. In all mouse genotypes, these ratios showed an increase before reaching a plateau, when a pseudodistributional equilibrium had been attained.

Steady-State Plasma and Brain Distribution of Sunitinib. An intraperitoneal infusion was used in the various genotypes to clearly elucidate the influence of active efflux by P-glycoprotein and Bcrp on the BBB penetration of sunitinib at steady state. In a system that exhibits linear distribution characteristics, the steady-state tissue-to-plasma concentration ratio should be equivalent to the tissue-to-plasma AUC ratio. The infusion was administered at a constant rate of 30 μg/h, and the plasma and brain concentrations were determined 48 hours (15–20 half-lives) after the start of infusion in wild-type, *Mdr1a/b(−/−)*, *Bcrp1(−/−)*, and *Mdr1a/b(−/−)Bcrp1(−/−)* mice. The steady-state plasma concentrations were not significantly different from each other in the four genotypes, and ranged from 0.195 (± 0.186) to 0.264 (± 0.086) μg/ml, another indication that P-gp and Bcrp do not influence the apparent clearance of sunitinib from plasma (Fig. 2A). This is in agreement with the single oral dose study in which the apparent clearance of sunitinib is also not altered by active efflux. However, the steady-state brain concentration in the wild-type mice was significantly lower (0.09 ± 0.07 μg/g) than that observed in the triple knockout mice (4.46 ± 1.66 μg/g; $P < 0.05$). When compared with wild-type mice, the brain steady-state concentrations were not different in the *Bcrp1(−/−)* mice (0.09 ± 0.04 μg/g), but were 4.3-fold higher in the *Mdr1a/b(−/−)* mice (0.39 ± 0.36 μg/g; $P < 0.05$) (Fig. 2B; Table 2). The steady-state brain-to-plasma ratio was 2.33 ± 0.56 in *Mdr1a/b(−/−)* mice and 0.73 ± 0.44 in *Bcrp1(−/−)* mice, whereas in the *Mdr1a/b(−/−)Bcrp1(−/−)* mice it was 17.44 ± 5.08, a 34-fold increase in sunitinib brain distribution when both of the transporters are absent. These steady-state data indicate that a single deletion of either P-gp or Bcrp does not impact sunitinib brain distribution to a great extent; however, deletion of both transporters results in a significant increase in sunitinib brain distribution (Fig. 2C). These results are in agreement with a previous report by Tang et al. (2012). The authors reported sunitinib brain distribution across the same genotypes of mice at a single time point (6 hours post oral dose). Since the efflux clearance from brain depends on the relevant efflux transporter expression [i.e., present (wild type) versus absent (transgenic knockout mice)], determination of the brain-to-plasma ratio at a single time point across genotypes may lead to significant errors, depending on the time point and the distribution kinetics of the drug (Wang, 2011). Furthermore, if the chosen time point does not represent a steady state, the brain-to-plasma ratio will change with time until pseudodistributional equilibrium is achieved in the terminal phase (see Fig. 1C). However, it is important to note that, after a single dose or intermittent multiple dosing, the steady-state condition for brain distribution can be approximated by a transient steady state in the brain, which will occur at a specific time that corresponds to the maximum concentration in the brain (peak brain concentration) relative to the plasma concentration at that same time (T_{max} of drug in brain). Tissue distribution at a single time point can, however, be determined at transient steady state, that is, when the drug concentration in the target tissue is at maximum. At this point, the rate of change of drug concentration in the target tissue, which in this case is the brain, is equal to zero, implying that the rate into the brain is at pseudo-distributional equilibrium with the rate out of the brain.

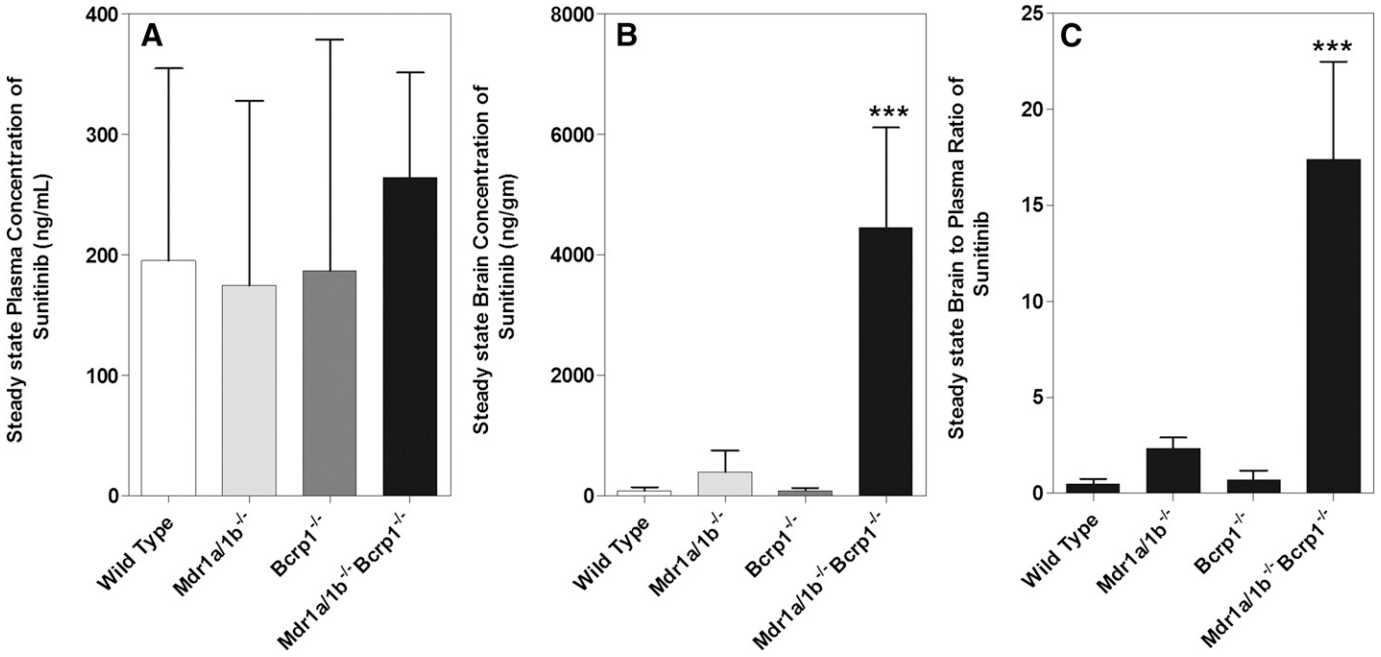

Fig. 2. (A) Steady-state plasma concentrations of sunitinib after a continuous intraperitoneal infusion at 30 μg/h for 48 hours in wild-type, *Mdr1a/b(−/−)*, *Bcrp1(−/−)*, and *Mdr1a/b(−/−)Bcrp1(−/−)* mice. (B) Corresponding steady-state brain concentrations of sunitinib in wild-type, *Mdr1a/b(−/−)*, *Bcrp1(−/−)*, and *Mdr1a/b(−/−)Bcrp1(−/−)* mice. (C) Steady-state brain-to-plasma ratios of sunitinib.

In our results, we observed that the steady-state brain-to-plasma concentration ratio ($C_{ss,\ brain}/C_{ss,\ plasma}$) in all four genotypes was similar to the corresponding brain-to-plasma partition coefficient (K_p) observed after oral dose (AUC_{brain}/AUC_{plasma}), which in turn was comparable to that obtained at transient steady state ($C_{brain,\ max}/C_{plasma}$) and at 1 hour post oral dose ($C_{brain,\ 1\ hour\ PO}/C_{plasma,\ 1\ hour\ PO}$) in all genotypes (Table 3).

Inhibition of P-gp and Bcrp Influences the Brain Distribution of Sunitinib. In the past, many research groups have used two approaches to delineate the contribution of efflux transporters in drug delivery to the central nervous system: 1) a genetic approach using genetic knockout transgenic mice, and 2) pharmacological inhibition of P-gp and Bcrp at the blood-brain barrier (Wang et al., 2012).

In this study, we compared the previous approaches by comparing the brain-to-plasma concentration ratio at 1 hour (plasma T_{max} in wild type; Table 1) after an oral dose of 20 mg/kg sunitinib in knockout mice [*Mdr1a/b(−/−)*, *Bcrp1(−/−)*, and *Mdr1a/b(−/−)Bcrp1(−/−)*] to the wild-type mice that were administered pharmacological inhibitors of these two efflux transporters. Genetic deletion of transporters resulted in a drug-targeting index at a single time point (1 hour) of 0.5-fold in Bcrp knockout mice, 3.7-fold in P-gp knockout mice, and 17.3-fold in triple knockout mice. Administration of pharmacological inhibitors did not influence the plasma concentration of sunitinib at this time point (Fig. 3A); however, significant differences were observed in the brain concentrations (Fig. 3B). A specific Bcrp inhibitor (Ko143, 10 mg/kg) and a specific P-gp inhibitor (zosuquidar, LY335979, 25 mg/kg) resulted in brain targeting increase of 0.9-fold and 3.5-fold, respectively. In addition, a 12-fold increase in brain targeting of sunitinib was observed upon administration of the dual P-gp/Bcrp inhibitor (elacridar, GF120918, 10 mg/kg). The brain targeting of sunitinib using these pharmacological inhibitors was comparable to that observed with the transgenic mice (Fig. 3C).

Importantly, the current study examines the effect of the specific P-gp inhibitor, zosuquidar, in *Bcrp1(−/−)* mice, and the specific Bcrp inhibitor, Ko-143, in *Mdr1a/b(−/−)* mice on sunitinib brain distribution. Further, simultaneous inhibition of P-gp and BCRP was achieved by administration of both zosuquidar and Ko143 to the FVB wild-type mice. The plasma and brain concentrations from these mice were determined at

TABLE 2

Steady-state plasma and brain concentrations of sunitinib in wild-type, *Mdr1a/b(−/−)*, *Bcrp1(−/−)*, and *Mdr1a/b(−/−)Bcrp1(−/−)* mice after a constant intraperitoneal infusion of sunitinib at a rate of 30 μg/h for 48 hours (n = 4 each group)

Data presented as the mean ± S.D.

Genotype	Plasma Css	Brain Css	Brain-to-Plasma Ratio
	$\mu g/ml$	$\mu g/g$	
FVB wild type	0.19 ± 0.16	0.09 ± 0.06	0.51 ± 0.26
Mdr1a/b(−/−)	0.18 ± 0.15	0.39 ± 0.36	2.33 ± 0.56[a]
Bcrp1(−/−)	0.19 ± 0.19	0.09 ± 0.04	0.73 ± 0.44
Mdr1a/b(−/−)Bcrp1(−/−)	0.26 ± 0.09	4.46 ± 1.66[a]	17.44 ± 5.08[a]

[a]$P < 0.005$ compared with wild type.

TABLE 3

Brain-to-plasma ratios of sunitinib in all genotypes after a single oral dose (20 mg/kg), steady-state concentration ratios after a continuous intraperitoneal infusion (rate equal to 30 μg/h), at transient steady state (calculated as the maximum brain concentration to the corresponding plasma concentration in each genotype), and concentration ratios determined at 1 hour post oral dose (20 mg/kg) in each genotype

Data are presented as the mean ± S.D.

Genotype	AUC_0^{∞}, PO	C_{ss} Steady State i.p.	Transient Steady State	Ratio at 1 h
FVB wild type	0.42	0.51 ± 0.26	0.66 ± 0.17	0.42 ± 0.09
Mdr1a/b(−/−)	1.61	2.33 ± 0.56	2.42 ± 1.42	1.76 ± 0.65
Bcrp1(−/−)	0.88	0.73 ± 0.44	1.09 ± 0.38	0.24 ± 0.20
Mdr1a/b(−/−)Bcrp1(−/−)	20.53	17.44 ± 5.08	12.83 ± 1.26	8.14 ± 3.47

PO, orally.

1 hour post oral dose of 20 mg/kg sunitinib. The brain-to-plasma ratio was 1.8 in *Mdr1a/b(−/−)* mice that received Ko143, whereas the brain-to-plasma ratio in *Bcrp1(−/−)* mice that received zosuquidar was 3.6. However, the cohort of wild-type mice that received both zosuquidar and Ko143 had a brain-to-plasma ratio of 3.7, whereas the group that received elacridar and *Mdr1a/b(−/−)Bcrp1(−/−)* mice had a brain-to-plasma ratio of 5.6 and 8.1, respectively (Fig. 3; Table 4).

These results show the correlation between the use of selective and dual pharmacological transport inhibitors and specific genetic deletion of transporters in the brain distribution of sunitinib. This agreement between the two approaches also indicates that, for sunitinib, it is likely that Ko143 and LY335979 are truly selective for the inhibition of Bcrp and P-gp, respectively. Moreover, in this regard, we have previously determined (Agarwal et al., 2012) via a quantitative proteomics approach that genetic deletion of P-gp and Bcrp does not influence the expression of several transport systems at the BBB, and P-gp and Bcrp do not compensate for the loss of one another by upregulation of the other's expression in the BBB.

Discussion

The objective of this study was to investigate and pharmacokinetically assess mechanisms that limit brain distribution of sunitinib for the treatment of GBM. Gliomas are fatal brain tumors characterized by a high degree of microvascular proliferation with endothelial cell migration. A highly invasive tumor, the cells have a strong tendency to migrate in other parts of the brain and hide behind an intact BBB (Agarwal et al., 2011b). It is therefore important to achieve adequate drug concentrations across the BBB, in the brain parenchyma, to target the tumor cells that reside in the growing edge of the tumor as well as in the distant sites of the brain. Previous preclinical investigations have suggested that efflux transporters, P-gp and Bcrp, limit the delivery of several anticancer agents into the brain. In the current study, we examined the influence of P-gp and Bcrp in restricting the brain distribution of sunitinib in the FVB strain [wild-type, *Mdr1a/b(−/−)*, *Bcrp1(−/−)*, and *Mdr1a/b(−/−)Bcrp1(−/−)* mice] using novel pharmacokinetic tissue distribution assessment methods, and proposed strategies to improve its delivery across the BBB based on efflux transport inhibition.

Sunitinib is a multitargeted tyrosine kinase inhibitor with activity against VEGFR1–3 and PDGFR-α/β, in addition to other regulators of tumor growth and angiogenesis (Christensen, 2007). As a pan-inhibitor of VEGFR, particularly VEGFR2, sunitinib represents an attractive treatment option as an antiangiogenic drug in the therapy of glioma. However, clinical trials using sunitinib (Neyns et al., 2011; Pan et al., 2012) and several molecularly targeted agents (e.g., cediranib, pazopanib, vandetanib) have been unsuccessful in GBM therapy (Batchelor et al., 2010; Iwamoto et al., 2010; Kreisl et al., 2012). This may be due in part to the limited delivery of these agents across the BBB (Minocha et al., 2012a,b; Wang et al., 2012).

To quantify the influence of efflux transporters, P-gp and Bcrp, on the brain distribution of sunitinib, we performed oral pharmacokinetic studies in FVB mice [wild-type, *Mdr1a/b(−/−)*, *Bcrp1(−/−)*, and *Mdr1a/b(−/−)Bcrp1(−/−)*]. Plasma and brain concentration-time profiles were determined in all four groups. $AUC_{0\text{-}\infty,\ plasma}$ values were not different among all four genotypes; however, $AUC_{0\text{-}\infty,\ brain}$ was different among all groups. Although sunitinib showed substantial partitioning into the brain (K_p = 0.42), deletion of both P-gp and Bcrp resulted in an AUC brain-to-plasma ratio of 20.5. Single deletion of P-gp or Bcrp had little influence on the brain distribution of sunitinib; however, a notable difference was observed in the absence of both transporters. This suggests that both P-gp and Bcrp act in a concerted fashion to limit the brain distribution of sunitinib (Fig. 1; Table 1). The DTI of sunitinib for the brain was 3.9 in *Mdr1a/b(−/−)* mice and 2.1 in *Bcrp1(−/−)* mice. The DTI in *Mdr1a/b(−/−)Bcrp1(−/−)* mice was 48.9, indicating a significant role of both P-gp and Bcrp in sunitinib's brain distribution.

Furthermore, to examine the penetration of sunitinib across the BBB, we determined the steady-state brain-to-plasma ratios ($C_{ss,\ brain}/C_{ss,\ plasma}$) in wild-type and transgenic transporter-deficient mice using a continuous intraperitoneal infusion lasting 48 hours. Although the plasma concentrations at steady state were not different among all groups, suggesting that the systemic distribution of sunitinib is not influenced by active efflux via P-gp and Bcrp, the steady-state brain concentrations were significantly greater in the group that lacked both P-gp and Bcrp ($P < 0.05$) (Fig. 2; Table 2). The steady-state brain-to-plasma ratios in wild-type, *Mdr1a/b(−/−)*, *Bcrp1(−/−)*, and *Mdr1a/b(−/−)Bcrp1(−/−)* mice were 0.51 ± 0.26, 2.33 ± 0.56, 0.73 ± 0.44, and 17.44 ± 5.08, respectively. These ratios are comparable to the corresponding AUC brain-to-plasma ratios determined after a single oral dose (Table 3).

Previously, Tang et al. (2012) reported the influence of P-gp and Bcrp on the brain distribution of sunitinib across the transporter-deleted genotypes of mice at 6 hours post single

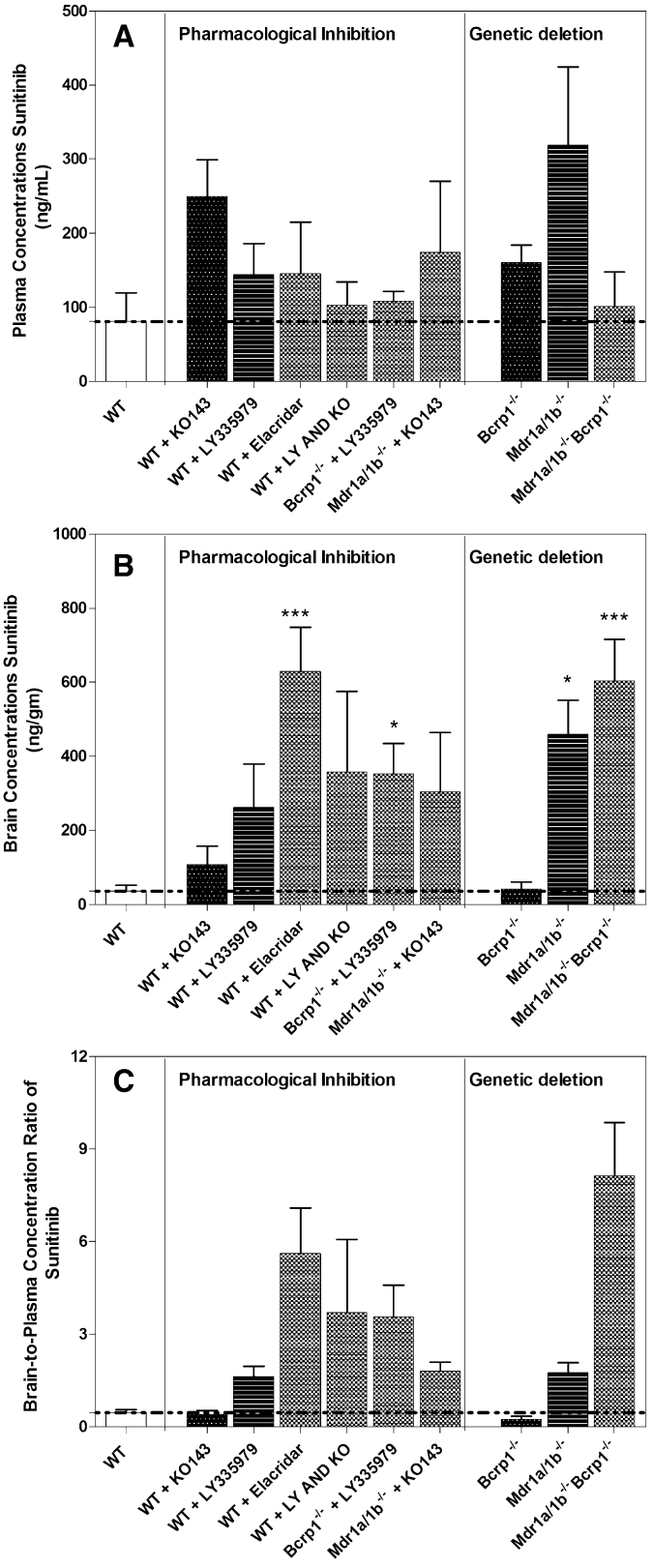

Fig. 3. (A) Plasma concentrations of sunitinib at 1 hour post oral dose (20 mg/kg) in wild-type (WT) mice after administration of a selective P-gp inhibitor [LY335979 (25 mg/kg)], selective Bcrp inhibitor [Ko143 (10 mg/kg)], both LY335979 and Ko143, and a dual P-gp/Bcrp inhibitor [elacridar (10 mg/kg)], selective P-gp inhibitor in *Bcrp1(−/−)* and selective Bcrp inhibitor in *Mdr1a/b(−/−)* mice. The plasma concentrations with pharmacological inhibition are compared at 1 hour in transgenic transporter-deficient mice. (B) Corresponding brain concentrations in the treatment group. (C) Brain-to-plasma ratios in corresponding treatment groups.

oral dose. Estimation of true drug partitioning into a tissue at a single time point can misguide interpretation of the effect of efflux transport on tissue distribution, depending on the chosen time point and the differences in the distributional kinetics of the drug under investigation. Characterization of brain distribution at a transient steady state can be considered to be an estimate of the steady-state tissue partitioning since it is at that point in time when the rate of drug entry into the brain is equal to the rate out of the brain (Table 3). Estimation of the brain-to-plasma distribution using a single time point before or after attainment of $C_{\max\ \mathrm{brain}}$ can lead to an under- or overestimation of the true tissue (brain) partition coefficient. Therefore, determining brain distribution at only one time point may be misleading depending on when the brain/plasma concentration ratio is determined, which is dependent on when the brain is sampled. Riad et al. (1993) have previously studied this "transient steady-state" approach for carbamazepine metabolites in humans. In our study, we found that the AUC brain-to-plasma ratio after a single oral dose was similar to both the steady-state brain-to-plasma ratio and the brain-to-plasma ratio at a transient steady state (Table 3).

Besides using transporter knockout mice, we also studied the effect of administering specific P-gp or Bcrp inhibitors and a dual inhibitor of P-gp and Bcrp on the plasma and brain concentration of sunitinib at 1 hour post oral dose of sunitinib. Results from this study indicated that plasma concentrations were not different at 1 hour in all treatment groups (Fig. 3A), and brain concentrations were not different in the cohorts that received specific P-gp inhibitor, zosuquidar, and specific Bcrp inhibitor, Ko143. However, a ~12-fold increase in the brain-to-plasma ratio was observed in the group of mice that received a dual P-gp and Bcrp inhibitor, elacridar. These findings were comparable to those observed with the knockout mice (Fig. 3, B and C; Table 4).

The results from this study warranted further investigation of the potential role of P-gp and Bcrp in mediating the active efflux of sunitinib from brain. To examine this, we administered a specific P-gp inhibitor to *Bcrp1(−/−)* mice and a specific Bcrp inhibitor to *Mdr1a/b(−/−)* mice. Additionally, we also administered both zosuquidar and Ko143 to wild-type mice and determined plasma and brain concentrations of sunitinib at 1 hour To the best of our knowledge, this is the first time that such an approach has been used to understand the role of P-gp and Bcrp in the distribution of sunitinib. The results from this study confirmed our results from the single oral dose study and steady-state distributional kinetics, i.e., that sunitinib is actively effluxed by both P-gp and Bcrp at the BBB. It is important to note here that the brain-to-plasma concentration ratio of sunitinib in the groups of mice receiving pharmacological inhibitors for both P-gp and Bcrp was not significantly different from the single knockout mice receiving specific P-gp or Bcrp inhibitor and the corresponding transgenic mice (Fig. 3C). The concordance between these approaches (use of transgenic mice versus pharmacological inhibitors) to determine the impact of efflux transport via P-gp and Bcrp on the brain distribution of sunitinib suggests

TABLE 4
Comparison of brain-to-plasma ratio of sunitinib in transgenic transporter deficient mice and in FVB wild-type mice treated with specific P-gp and/or Bcrp inhibitors
Values are the mean ± S.D.

Pharmacological Inhibition		Genetic Deletion	
Wild type	0.47 ± 0.18	Wild type	0.47 ± 0.18
Wild type + LY335979	1.64 ± 0.57	*Mdr1a/b(−/−)*	1.76 ± 0.65
Wild type + Ko143	0.42 ± 0.24	*Bcrp1(−/−)*	0.24 ± 0.20
Wild type + elacridar	5.63 ± 2.33	*Mdr1a/b(−/−)Bcrp1(−/−)*	8.14 ± 3.47
Wild type + LY335979 + Ko143	3.71 ± 2.37	*Mdr1a/b(−/−)Bcrp1(−/−)*	8.14 ± 3.47
Mdr1a/b(−/−) + Ko143	1.81 ± 0.59	*Mdr1a/b(−/−)Bcrp1(−/−)*	8.14 ± 3.47
Bcrp1(−/−) + LY335979	3.56 ± 2.08	*Mdr1a/b(−/−)Bcrp1(−/−)*	8.14 ± 3.47

that pharmacological inhibition can be used as an effective tool to improve the brain distribution of sunitinib for the treatment of glioma. Recently, Kunimatsu et al. (2013) reported a similar phenomenon on greater accumulation in the brain on dual inhibition of efflux transport in rats. This is important since tailored chemotherapy with sunitinib in an anaplastic meningioma patient expressing PDGFR-β failed to show desirable efficacy (Yoshikawa et al., 2012). Therefore, it is important to understand that, in addition to the intended molecular target, issues related to effective drug delivery are pertinent in the treatment of brain tumor.

In conclusion, we have shown that sunitinib has limited penetration into the brain due to the presence of efflux transport mediated by both P-gp and Bcrp at the BBB. Single deletion of P-gp or Bcrp does not play a significant role as compared with dual P-gp and Bcrp deletion, indicating a simple functional compensation between these two transporters at the BBB in restricting the brain distribution of sunitinib (Enokizono et al., 2008; Kodaira et al., 2010). We also showed here that the tissue partition coefficient obtained after a single oral dose, calculated by the AUC brain-to-plasma ratio, is similar to the brain-to-plasma steady-state concentration ratios, which would be expected for nonsaturable, linear distributional kinetics. Furthermore, determination of the extent of brain distribution of sunitinib can be determined at a single time point, provided that the chosen time point is the time in which a transient steady state is attained between the plasma and the brain. This will occur at a time when the brain concentration reaches a maximum following a single dose. Relying on a single time point not at this transient steady state to determine the brain partition coefficient can lead to significant errors, and complicate the comparison of several studies. Moreover, administration of selective inhibitors of active efflux as well as dual inhibitors of efflux transporters resulted in enhanced brain penetration of sunitinib, in concordance with that observed in transgenic mice. These results can be of clinical significance to improve the brain delivery of sunitinib to areas of tumor cells that lie hidden behind an intact BBB that has active P-gp and Bcrp transport systems.

Authorship Contributions

Participated in research design: Oberoi, Mittapalli, Elmquist.
Conducted experiments: Oberoi, Mittapalli.
Performed data analysis: Oberoi, Mittapalli, Elmquist.
Wrote or contributed to the writing of the manuscript: Oberoi, Mittapalli, Elmquist.

References

Agarwal S and Elmquist WF (2012) Insight into the cooperation of P-glycoprotein (ABCB1) and breast cancer resistance protein (ABCG2) at the blood-brain barrier: a case study examining sorafenib efflux clearance. *Mol Pharm* **9**:678–684.

Agarwal S, Hartz AM, Elmquist WF, and Bauer B (2011a) Breast cancer resistance protein and P-glycoprotein in brain cancer: two gatekeepers team up. *Curr Pharm Des* **17**:2793–2802.

Agarwal S, Manchanda P, Vogelbaum MA, Ohlfest JR, and Elmquist WF (2013) Function of the blood-brain barrier and restriction of drug delivery to invasive glioma cells: findings in an orthotopic rat xenograft model of glioma. *Drug Metab Dispos* **41**:33–39.

Agarwal S, Sane R, Oberoi R, Ohlfest JR, and Elmquist WF (2011b) Delivery of molecularly targeted therapy to malignant glioma, a disease of the whole brain. *Expert Rev Mol Med* **13**:e17.

Agarwal S, Sane R, Ohlfest JR, and Elmquist WF (2011c) The role of the breast cancer resistance protein (ABCG2) in the distribution of sorafenib to the brain. *J Pharmacol Exp Ther* **336**:223–233.

Agarwal S, Uchida Y, Mittapalli RK, Sane R, Terasaki T, and Elmquist WF (2012) Quantitative proteomics of transporter expression in brain capillary endothelial cells isolated from P-glycoprotein (P-gp), breast cancer resistance protein (Bcrp), and P-gp/Bcrp knockout mice. *Drug Metab Dispos* **40**:1164–1169.

Allen JD, van Loevezijn A, Lakhai JM, van der Valk M, van Tellingen O, Reid G, Schellens JH, Koomen GJ, and Schinkel AH (2002) Potent and specific inhibition of the breast cancer resistance protein multidrug transporter in vitro and in mouse intestine by a novel analogue of fumitremorgin C. *Mol Cancer Ther* **1**:417–425.

Batchelor TT, Duda DG, di Tomaso E, Ancukiewicz M, Plotkin SR, Gerstner E, Eichler AF, Drappatz J, Hochberg FH, and Benner T, et al. (2010) Phase II study of cediranib, an oral pan-vascular endothelial growth factor receptor tyrosine kinase inhibitor, in patients with recurrent glioblastoma. *J Clin Oncol* **28**:2817–2823.

Brem S, Tsanaclis AM, Gately S, Gross JL, and Herblin WF (1992) Immunolocalization of basic fibroblast growth factor to the microvasculature of human brain tumors. *Cancer* **70**:2673–2680.

Chen Y, Agarwal S, Shaik NM, Chen C, Yang Z, and Elmquist WF (2009) P-glycoprotein and breast cancer resistance protein influence brain distribution of dasatinib. *J Pharmacol Exp Ther* **330**:956–963.

Christensen JG (2007) A preclinical review of sunitinib, a multitargeted receptor tyrosine kinase inhibitor with anti-angiogenic and antitumour activities. *Ann Oncol* **18**:x3–10.

Cohen MH, Shen YL, Keegan P, and Pazdur R (2009) FDA drug approval summary: bevacizumab (Avastin) as treatment of recurrent glioblastoma multiforme. *Oncologist* **14**:1131–1138.

Dai CL, Liang YJ, Wang YS, Tiwari AK, Yan YY, Wang F, Chen ZS, Tong XZ, and Fu LW (2009) Sensitization of ABCG2-overexpressing cells to conventional chemotherapeutic agent by sunitinib was associated with inhibiting the function of ABCG2. *Cancer Lett* **279**:74–83.

Dai H, Marbach P, Lemaire M, Hayes M, and Elmquist WF (2003) Distribution of STI-571 to the brain is limited by P-glycoprotein-mediated efflux. *J Pharmacol Exp Ther* **304**:1085–1092.

de Bruijn P, Sleijfer S, Lam MH, Mathijssen RH, Wiemer EA, and Loos WJ (2010) Bioanalytical method for the quantification of sunitinib and its n-desethyl metabolite SU12662 in human plasma by ultra performance liquid chromatography/tandem triple-quadrupole mass spectrometry. *J Pharm Biomed Anal* **51**:934–941.

di Tomaso E, Snuderl M, Kamoun WS, Duda DG, Auluck PK, Fazlollahi L, Andronesi OC, Frosch MP, Wen PY, and Plotkin SR, et al. (2011) Glioblastoma recurrence after cediranib therapy in patients: lack of "rebound" revascularization as mode of escape. *Cancer Res* **71**:19–28.

Dudek AZ, Raza A, Chi M, Singhal M, Oberoi R, Mittapalli RK, Agarwal S, and Elmquist WF (2013) Brain metastases from renal cell carcinoma in the era of tyrosine kinase inhibitors. *Clin Genitourin Cancer* **11**:155–160.

Enokizono J, Kusuhara H, Ose A, Schinkel AH, and Sugiyama Y (2008) Quantitative investigation of the role of breast cancer resistance protein (Bcrp/Abcg2) in limiting brain and testis penetration of xenobiotic compounds. *Drug Metab Dispos* **36**:995–1002.

Faivre S, Demetri G, Sargent W, and Raymond E (2007) Molecular basis for sunitinib efficacy and future clinical development. *Nat Rev Drug Discov* **6**:734–745.

Horowitz M, Blasberg R, Molnar P, Strong J, Kornblith P, Pleasants R, and Fenstermacher J (1983) Regional [14C]misonidazole distribution in experimental RT-9 brain tumors. *Cancer Res* **43**:3800–3807.

Hu S, Chen Z, Franke R, Orwick S, Zhao M, Rudek MA, Sparreboom A, and Baker SD (2009) Interaction of the multikinase inhibitors sorafenib and sunitinib with solute carriers and ATP-binding cassette transporters. *Clin Cancer Res* **15**:6062–6069.

Hubensack M, Müller C, Höcherl P, Fellner S, Spruss T, Bernhardt G, and Buschauer A (2008) Effect of the ABCB1 modulators elacridar and tariquidar on the distribution of paclitaxel in nude mice. *J Cancer Res Clin Oncol* **134**:597–607.

Iwamoto FM, Lamborn KR, Robins HI, Mehta MP, Chang SM, Butowski NA, Deangelis LM, Abrey LE, Zhang WT, and Prados MD, et al. (2010) Phase II trial of pazopanib (GW786034), an oral multi-targeted angiogenesis inhibitor, for adults with recurrent glioblastoma (North American Brain Tumor Consortium Study 06-02). *Neuro-oncol* **12**:855–861.

Kodaira H, Kusuhara H, Ushiki J, Fuse E, and Sugiyama Y (2010) Kinetic analysis of the cooperation of P-glycoprotein (P-gp/Abcb1) and breast cancer resistance protein (Bcrp/Abcg2) in limiting the brain and testis penetration of erlotinib, flavopiridol, and mitoxantrone. *J Pharmacol Exp Ther* **333**:788–796.

Kreisl TN, McNeill KA, Sul J, Iwamoto FM, Shih J, and Fine HA (2012) A phase I/II trial of vandetanib for patients with recurrent malignant glioma. *Neuro-oncol* **14**: 1519–1526.

Kunimatsu S, Mizuno T, Fukudo M, and Katsura T (2013) Effect of P-glycoprotein and breast cancer resistance protein inhibition on the pharmacokinetics of sunitinib in rats. *Drug Metab Dispos* **41**:1592–1597.

Lagas JS, van Waterschoot RA, van Tilburg VA, Hillebrand MJ, Lankheet N, Rosing H, Beijnen JH, and Schinkel AH (2009) Brain accumulation of dasatinib is restricted by P-glycoprotein (ABCB1) and breast cancer resistance protein (ABCG2) and can be enhanced by elacridar treatment. *Clin Cancer Res* **15**:2344–2351.

Levin VA, Freeman-Dove M, and Landahl HD (1975) Permeability characteristics of brain adjacent to tumors in rats. *Arch Neurol* **32**:785–791.

Louis DN, Ohgaki H, Wiestler OD, Cavenee WK, Burger PC, Jouvet A, Scheithauer BW, and Kleihues P (2007) The 2007 WHO classification of tumours of the central nervous system. *Acta Neuropathol* **114**:97–109.

Maliepaard M, van Gastelen MA, Tohgo A, Hausheer FH, van Waardenburg RC, de Jong LA, Pluim D, Beijnen JH, and Schellens JH (2001) Circumvention of breast cancer resistance protein (BCRP)-mediated resistance to camptothecins in vitro using non-substrate drugs or the BCRP inhibitor GF120918. *Clin Cancer Res* **7**: 935–941.

Minocha M, Khurana V, Qin B, Pal D, and Mitra AK (2012a) Co-administration strategy to enhance brain accumulation of vandetanib by modulating P-glycoprotein (P-gp/Abcb1) and breast cancer resistance protein (Bcrp1/Abcg2) mediated efflux with m-TOR inhibitors. *Int J Pharm* **434**:306–314.

Minocha M, Khurana V, Qin B, Pal D, and Mitra AK (2012b) Enhanced brain accumulation of pazopanib by modulating P-gp and Bcrp1 mediated efflux with canertinib or erlotinib. *Int J Pharm* **436**:127–134.

Nedelman JR and Jia X (1998) An extension of Satterthwaite's approximation applied to pharmacokinetics. *J Biopharm Stat* **8**:317–328.

Neyns B, Sadones J, Chaskis C, Dujardin M, Everaert H, Lv S, Duerinck J, Tynninen O, Nupponen N, and Michotte A, et al. (2011) Phase II study of sunitinib malate in patients with recurrent high-grade glioma. *J Neurooncol* **103**:491–501.

Oberoi RK, Mittapalli RK, Fisher J, and Elmquist WF (2013) Sunitinib LC–MS/MS assay in mouse plasma and brain tissue: application in CNS distribution studies. *Chromatographia* DOI 10.1007/s10337-013-2528-1.

Pan E, Yu D, Yue B, Potthast L, Chowdhary S, Smith P, and Chamberlain M (2012) A prospective phase II single-institution trial of sunitinib for recurrent malignant glioma. *J Neurooncol* **110**:111–118.

Poller B, Iusuf D, Sparidans RW, Wagenaar E, Beijnen JH, and Schinkel AH (2011) Differential impact of P-glycoprotein (ABCB1) and breast cancer resistance protein (ABCG2) on axitinib brain accumulation and oral plasma pharmacokinetics. *Drug Metab Dispos* **39**:729–735.

Polli JW, Olson KL, Chism JP, John-Williams LS, Yeager RL, Woodard SM, Otto V, Castellino S, and Demby VE (2009) An unexpected synergist role of P-glycoprotein and breast cancer resistance protein on the central nervous system penetration of the tyrosine kinase inhibitor lapatinib (N-3-chloro-4-[(3-fluorobenzyl)oxy]phenyl-6-[5-([2-(methylsulfonyl)ethyl]aminomethyl)-2-furyl]-4-quinazolinamine; GW572016). *Drug Metab Dispos* **37**:439–442.

Riad LE, Chan KK, and Sawchuk RJ (1993) Transient steady-state analysis: application in the determination of the relative formation and elimination clearances of two major carbamazepine metabolites in humans. *Pharm Res* **10**:1090–1092.

Shepard RL, Cao J, Starling JJ, and Dantzig AH (2003) Modulation of P-glycoprotein but not MRP1- or BCRP-mediated drug resistance by LY335979. *Int J Cancer* **103**: 121–125.

Shukla S, Robey RW, Bates SE, and Ambudkar SV (2009) Sunitinib (Sutent, SU11248), a small-molecule receptor tyrosine kinase inhibitor, blocks function of the ATP-binding cassette (ABC) transporters P-glycoprotein (ABCB1) and ABCG2. *Drug Metab Dispos* **37**:359–365.

Tang SC, Lagas JS, Lankheet NA, Poller B, Hillebrand MJ, Rosing H, Beijnen JH, and Schinkel AH (2012) Brain accumulation of sunitinib is restricted by P-glycoprotein (ABCB1) and breast cancer resistance protein (ABCG2) and can be enhanced by oral elacridar and sunitinib coadministration. *Int J Cancer* **130**: 223–233.

Tuettenberg J, Friedel C, and Vajkoczy P (2006) Angiogenesis in malignant glioma—a target for antitumor therapy? *Crit Rev Oncol Hematol* **59**:181–193.

Wang T (2011) Mechanisms and analysis of the CNS distribution of cediranib, a molecularly-targeted anti-angiogenic agent, in pp 1 online resource (xi, 225 p.). http://conservancy.umn.edu/bitstream/116534/1/Wang_umn_0130E_12215.pdf.

Wang T, Agarwal S, and Elmquist WF (2012) Brain distribution of cediranib is limited by active efflux at the blood-brain barrier. *J Pharmacol Exp Ther* **341**: 386–395.

Wick W, Weller M, Weiler M, Batchelor T, Yung AW, and Platten M (2011) Pathway inhibition: emerging molecular targets for treating glioblastoma. *Neuro-oncol* **13**: 566–579.

Wong ML, Prawira A, Kaye AH, and Hovens CM (2009) Tumour angiogenesis: its mechanism and therapeutic implications in malignant gliomas. *J Clin Neurosci* **16**: 1119–1130.

Yoshikawa A, Nakada M, Ohtsuki S, Hayashi Y, Obuchi W, Sato Y, Ikeda C, Watanabe T, Kawahara Y, and Hasegawa T, et al. (2012) Recurrent anaplastic meningioma treated by sunitinib based on results from quantitative proteomics. *Neuropathol Appl Neurobiol* **38**:105–110.

Zhou Q and Gallo JM (2009) Differential effect of sunitinib on the distribution of temozolomide in an orthotopic glioma model. *Neuro-oncol* **11**:301–310.

Zhou Q, Guo P, and Gallo JM (2008) Impact of angiogenesis inhibition by sunitinib on tumor distribution of temozolomide. *Clin Cancer Res* **14**:1540–1549.

Address correspondence to: William F. Elmquist, Department of Pharmaceutics, University of Minnesota, 9-177 Weaver-Densford Hall, 308 Harvard Street SE, Minneapolis, MN 55455. E-mail: elmqu011@umn.edu